International Core Journal of Engineering Volume 12 Issue 3, 2026
ISSN: 2414-1895 DOI: 10.6919/ICJE.202603_12(3).0043

Investigation of the Laser Processing Mechanism of Tooth-Surface Texturing in PEEK-Based Involute Splines

Chen Wang[1], Xiangzhen Xue[1,*], Li Xiao[1], Zhongrong Wang[2], Zhaopeng Wu[1]

[1] College of Mechanical and Electrical Engineering, Shaanxi University of Science and Technology, Xi'an 710021, China

[2] AECC Sichuan Gas Turbine Establishment, Chengdu 610500, Sichuan, China

[*]Corresponding author. E-mail address: xuexiangzhen@sust.edu.cn

Abstract

To reveal the response behavior and formation mechanism of femtosecond laser-induced microtextures on the tooth surfaces of PEEK-based involute splines, this study selected three materials, namely PEEK5600G, PEEK5600LF30, and PEEK5600CF30. An orthogonal experimental design was adopted to systematically investigate the effects of laser average power, scanning speed, and number of scans on texture depth and width. The processed surfaces were characterized in terms of three-dimensional morphology using a DSX510 digital microscope. The experimental data were further processed, verified, and statistically analyzed using MATLAB and Origin. The results showed that the texture depth of all three materials was mainly governed by laser power. However, the three materials exhibited different response characteristics. For PEEK5600G, the texture depth was significantly affected by both laser power and scanning speed. For PEEK5600CF30, the texture depth was mainly controlled by laser power. In contrast, PEEK5600LF30 showed high sensitivity to laser power, scanning speed, and number of scans. The variation in texture width showed clear material dependence. For PEEK5600G, the texture width was mainly affected by laser power. For PEEK5600CF30, it was mainly influenced by scanning speed and number of scans. PEEK5600LF30 was sensitive to all three factors. Meanwhile, microscopic morphology analysis further showed that all three PEEK-based materials exhibited a competing material removal mechanism of ablation and melting under femtosecond laser irradiation. Ablation dominated in the central region of the groove, whereas a recast layer and molten material accumulation tended to form at the edges. Differences in the reinforcing components led to different thermophysical response characteristics, which ultimately resulted in significant differences in groove profile, edge quality, and parameter sensitivity.

Keywords

Involute Spline; PEEK-based Materials; Femtosecond Laser; Surface Microtexture.

1. Introduction

Involute splines are widely used in aerospace transmissions, high-end equipment, and heavy-duty connection systems because of their high load-carrying capacity, good centering performance, smooth power transmission, and tolerance for certain assembly deviations. During service, they are often subjected to complex combined loads, including torque, axial load, bending moment, and misalignment. The contact state of the tooth surfaces is characterized by the coexistence of rolling, sliding, and microslip. This condition can readily cause local stress concentration and relative slip,

ISSN: 2414-1895 DOI: 10.6919/ICJE.202603_12(3).0043

which in turn induce fretting wear, surface damage, and contact fatigue, ultimately reducing transmission accuracy, connection reliability, and service life. Therefore, improving the tribological behavior of spline tooth surfaces and delaying wear failure has become an important research focus in this field [1–2].

Studies have shown that properly designed surface textures can not only store and supply lubricant, trap wear debris, and reduce third-body wear, but also regulate the real contact state and local hydrodynamic effects under certain conditions. As a result, they can improve interfacial lubrication and reduce friction and wear. Compared with conventional methods such as mechanical machining, photolithography, and electrical discharge machining, laser surface texturing offers several advantages, including non-contact processing, high flexibility, high efficiency, low contamination, and precise control of pattern size and distribution. It has therefore become an important approach for surface functionalization. In particular, femtosecond lasers, with their ultrashort pulse duration, high peak power, and minimal heat-affected zone, are more suitable for the precise fabrication of microstructures on polymer and composite surfaces, while reducing the risk of thermal damage and maintaining high machining accuracy [3–7].

However, PEEK-based involute splines are made of non-metallic materials and therefore differ fundamentally from conventional metallic components. Existing studies have shown that pure PEEK still exhibits wear sensitivity under complex friction conditions. Although the addition of reinforcing or lubricating components such as carbon fiber, glass fiber, or PTFE can improve the mechanical or tribological properties of the material, it can also markedly alter its thermal conduction behavior, interfacial transfer film formation, and response to laser energy. As a result, different PEEK-based materials exhibit significant differences in both surface texturing behavior and tribological performance during service [8–11].

Although previous studies have systematically revealed the mechanisms by which surface microtextures improve tribological performance and have laid a foundation for their application in transmission components, several limitations remain. First, most existing studies have focused on traditional metallic materials, such as steels and alloys, whereas research on PEEK-based polymers remains relatively limited. The interaction mechanism between lasers and polymers differs fundamentally from that between lasers and metals, and therefore processing theories developed for metallic materials cannot be directly applied. Second, in the limited studies related to PEEK, most attention has been paid to microstructure fabrication on flat specimens, wettability regulation, or general tribological behavior. Some researchers have explored laser microtexturing of gear components or laser surface modification of PEEK, which provides useful references for spline-related studies. However, for PEEK-based involute spline pairs with complex curved tooth surfaces, there is still a lack of systematic understanding of how femtosecond laser parameters affect microtexture quality and how different material compositions lead to distinct response mechanisms. [12–14].

Therefore, this study selected three representative PEEK-based materials, namely PEEK5600G, PEEK5600LF30, and PEEK5600CF30, and fabricated groove-shaped microtextures on their involute spline tooth surfaces. An orthogonal experimental design was employed to systematically investigate the quantitative effects of laser average power, scanning speed, and number of scans on texture depth and width. Combined with three-dimensional morphology characterization and statistical analysis, the material removal behavior and formation mechanism of femtosecond laser processing under different reinforcing conditions were further clarified. This work aims to provide a solid theoretical basis and experimental reference for tooth-surface texturing design and process parameter optimization of PEEK-based involute spline pairs.

ISSN: 2414-1895 DOI: 10.6919/ICJE.202603_12(3).0043

2. Orthogonal Experimental Design for Laser Processing

2.1 Laser Processing Equipment and Experimental Preparation

Common surface microtexturing techniques include photolithography, focused ion beam micromachining, electrical discharge machining, chemical vapor deposition, and laser processing. Among these methods, laser processing is regarded as an ideal technique for surface microtexture fabrication because of its high efficiency, high precision, and low contamination.

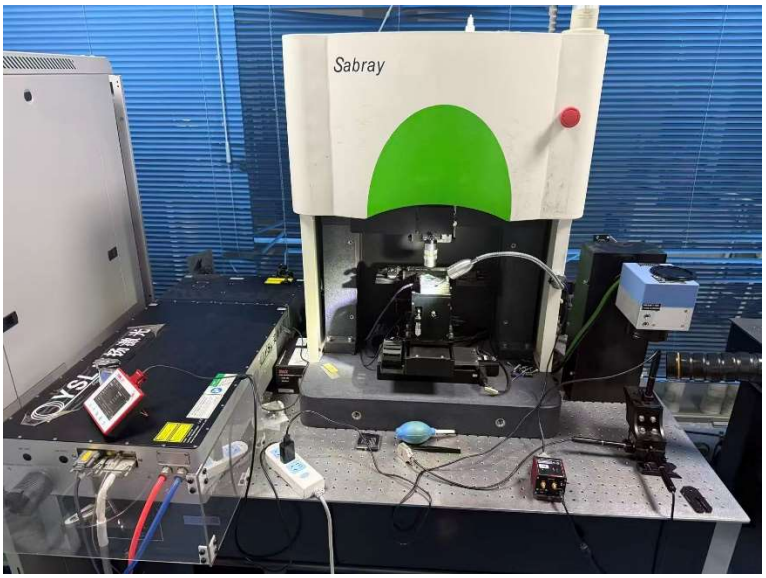

Figure 1. Femtosecond laser system

A FemtoYL-40 femtosecond laser system was used for microtexture fabrication in this study, and its main technical parameters are listed in Table 1.

Table 1. Main technical parameters of the FemtoYL-40 femtosecond laser system

Laser Parameter	Value
Average power (W)	19.97
Pulse width (fs)	270
Central wavelength (nm)	515.61
Spot diameter (um)	2.470
Repetition rate (kHz)	100
Beam quality	$M^2 < 1.3$

The test specimens were made of three PEEK-based materials, namely PEEK5600G, PEEK5600LF30, and PEEK5600CF30. The machined spline pair specimens are shown in Figure 2.

Before laser processing, all specimens were cleaned in an ultrasonic cleaner for 15 min using anhydrous ethanol as the cleaning medium. The operating frequency was set to 40 kHz, and the power density was adjusted to 0.3 W/cm² to remove possible surface contaminants such as dirt, grease, and oxides. The laser power was then calibrated, as shown in Figure 3(a), to ensure stable laser output and compliance with the processing requirements. Insufficient laser power may result in inadequate energy input and failure to produce the desired texture morphology, whereas excessive power may cause overmelting or expansion of the heat-affected zone, thereby deteriorating the surface quality.

ISSN: 2414-1895 DOI: 10.6919/ICJE.202603_12(3).0043

Therefore, careful adjustment of the laser power is essential for obtaining the expected texture depth and width while minimizing thermal effects and ensuring surface finish and processing consistency. Finally, the focal position was adjusted using a KDC101 electronic translation stage, as shown in Figure 3(b), to ensure accurate focusing of the laser beam on the material surface. An excessively long focal length may lead to beam divergence and inaccurate irradiation of the target area, whereas an excessively short focal length may cause excessive local energy concentration and localized damage. Precise adjustment of the focal position enabled the laser beam to remain accurately focused during each scan, thereby producing uniform and fine textures, avoiding focal offset, ensuring consistency of the processed area, reducing expansion of the heat-affected zone, and improving machining accuracy and surface quality.

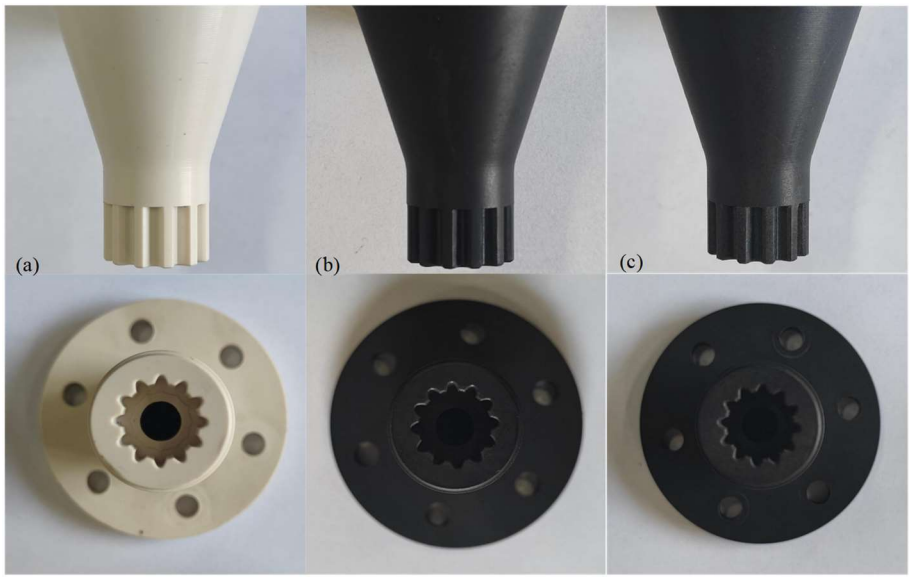

Figure 2. Machined specimens of the spline pair
(a) PEEK5600G; (b) PEEK5600LF30; (c) PEEK5600CF30

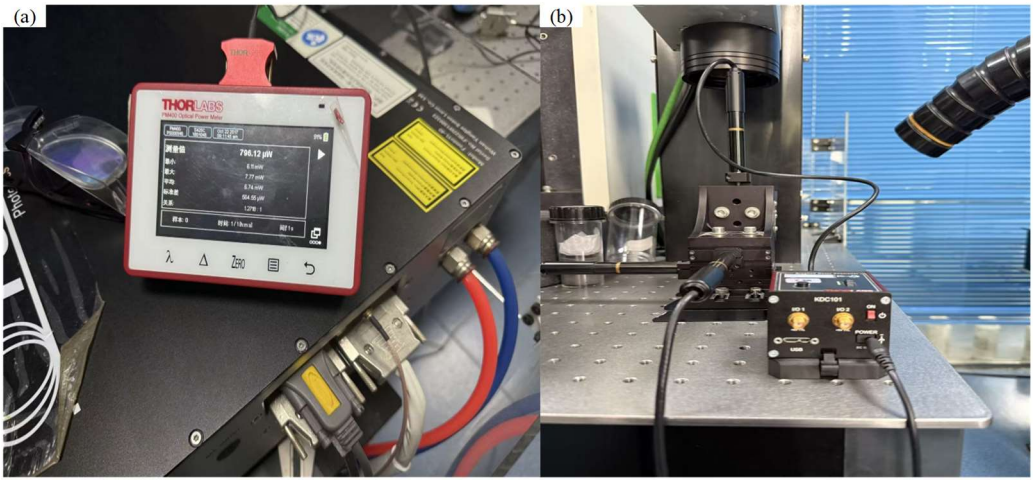

Figure 3. (a) laser calibration controller; (b) KDC101 electronic translation stage.

2.2 Selection of the Tooth Surface Texture

In mechanical transmission systems, involute spline pairs mainly serve to transmit torque and connect the shaft and hub. Their tooth surface meshing conditions are complex and are usually accompanied by high contact stress and multiple forms of relative motion during service. In most cases, several teeth carry the load simultaneously or alternately. Therefore, tooth surface contact involves not only rolling, but also sliding and microslip. Under the combined effects of backlash, fitting errors, and

ISSN: 2414-1895 DOI: 10.6919/ICJE.202603_12(3).0043

axial, radial, and angular displacements, local frictional slip can readily occur on the tooth surfaces, thereby aggravating wear. Meanwhile, because the space between spline teeth is limited, lubricant supply and replenishment are restricted. Under high-speed, heavy-load, and variable-load conditions, the lubricating film in the contact zone may become thinner or even break down, causing the tooth surfaces to remain under boundary or mixed lubrication for extended periods. In addition, if wear particles generated during meshing cannot be removed in time, they may induce abrasive wear and third-body wear, thereby reducing the service reliability of the transmission pair [15–17].

Based on the above characteristics, groove-shaped surface textures were selected for fabrication on the tooth surfaces of the involute spline pair in this study. Groove textures exhibit clear directionality and continuity, and can be arranged along the main sliding or contact direction of the tooth surface. During meshing, they can form relatively continuous lubricant transport channels, which facilitate lubricant entry into the contact region and promote lubricating film formation, thereby improving the lubrication state of the tooth surfaces and reducing friction and wear. At the same time, the grooves can provide discharge paths for wear particles and debris, reducing their accumulation in the contact zone and mitigating third-body wear. From the perspective of processing, groove textures are well matched with laser fabrication, allowing precise control of groove width, depth, spacing, and orientation. They also provide high processing repeatability and preserve a large proportion of the tooth surface load-bearing area while offering fluid transport channels. Therefore, groove-shaped surface textures were adopted on the tooth surfaces of the involute spline pair in this study [18–20].

2.3 Orthogonal Experimental Design

Orthogonal experimental design is an efficient multi-factor, multi-level method that enables systematic analysis of the effects of different factors on processing performance with a limited number of experiments. It is therefore well suited for identifying the factors that significantly affect the target responses and for determining their optimal level combinations. By using this method, the effects of laser power, scanning speed, and number of scans on groove depth and width can be comprehensively evaluated while reducing experimental cost and improving experimental efficiency.

Based on the literature review and preliminary experimental results, laser average power (P), scanning speed (V), and number of scans (N) were identified as the key factors affecting groove morphology and were therefore included in the orthogonal experimental design. The factor levels were determined by considering both published studies and practical processing experience, with the aim of covering a reasonable parameter range within a limited experimental scale and obtaining an optimal combination of processing parameters. In this study, an L25 (5^3) orthogonal array was employed, and a total of 25 experiments were conducted to systematically investigate the effects of different parameter combinations on groove fabrication quality.

The selection of factors and levels was based on previous literature and experimental experience [21–23], ensuring that the experiments covered the key factors that may influence texture morphology and providing reliable experimental data for subsequent optimization. The laser parameter settings and the orthogonal experimental design are presented in Tables 2 and 3.

Table 2. Laser parameter settings

Parameter	Value
Average power (W)	0.3, 0.4, 0.5, 0.6, 0.7
Scanning speed (mm/s)	40, 60, 80, 100, 120
Number of scans	1, 2, 3, 4, 5

ISSN: 2414-1895 DOI: 10.6919/ICJE.202603_12(3).0043

Table 3. Orthogonal experimental design of laser parameters

Experimental run number	Average power (W)	Scanning speed (mm/s)	Number of scans
F1	0.3	40	1
F2	0.3	60	3
F3	0.3	80	5
F4	0.3	100	2
F5	0.3	120	4
F6	0.4	40	5
F7	0.4	60	2
F8	0.4	80	4
F9	0.4	100	1
F10	0.4	120	3
F11	0.5	40	4
F12	0.5	60	1
F13	0.5	80	3
F14	0.5	100	5
F15	0.5	120	2
F16	0.6	40	3
F17	0.6	60	5
F18	0.6	80	2
F19	0.6	100	4
F20	0.6	120	1
F21	0.7	40	2
F22	0.7	60	4
F23	0.7	80	1
F24	0.7	100	3
F25	0.7	120	5

2.4 Data Measurement Methods

After laser processing, the specimens were first ultrasonically cleaned to ensure the reliability of subsequent morphology characterization. This step was intended to remove dust, remelted and resolidified debris, and other contaminants generated during processing and attached to the surface, thereby avoiding interference with three-dimensional reconstruction and parameter extraction. After cleaning and drying, a DSX510 digital microscope (Figure 4, Olympus) was used to scan the three-dimensional surface morphology of the textured region and obtain surface height field data.

As shown in Figure 5, the microscopic images acquired by the DSX system can be reconstructed into three-dimensional surface morphologies using the DSX image processing software, thereby enabling quantitative measurement. After the “profile measurement” function was selected in the software, geometric information such as depth and width at a given cross-section could be obtained directly by manually selecting the measurement position. To reduce random error in a single measurement and improve data representativeness, five different positions on the same specimen were selected for repeated measurements in each experimental group, and the three-dimensional scan data from each position were exported separately as CSV files. Considering that manual cross-section selection, baseline fitting, and data reading may introduce subjective errors, the five CSV files from each group were further imported into MATLAB for unified processing. An automated program was developed to perform standardized data processing and feature extraction under consistent baseline constraints, and key parameters such as texture depth, width, and ridge height were then calculated and statistically summarized from the repeated measurements.

ISSN: 2414-1895 DOI: 10.6919/ICJE.202603_12(3).0043

Figure 4. DSX510 digital microscope

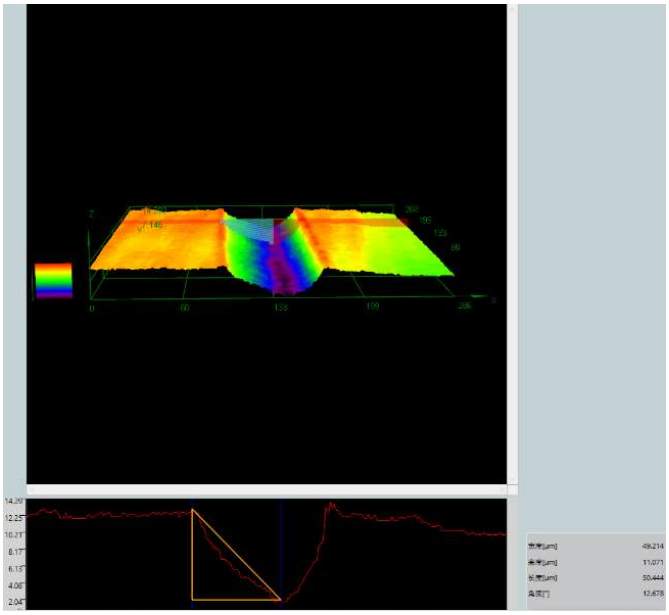

Figure 5. Measurement of texture data

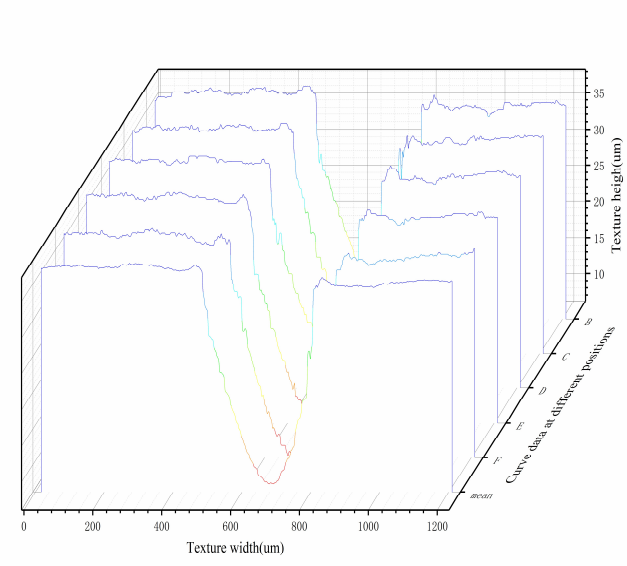

Figure 6. Verification of texture data

ISSN: 2414-1895 DOI: 10.6919/ICJE.202603_12(3).0043

When obvious outliers or large data dispersion were observed in the measurement results, the five datasets of that group were further imported into Origin to generate three-dimensional morphology maps (Figure 6). This was done to visually re-examine abnormal regions and to perform manual verification, thereby providing secondary validation of the measurement results and ensuring the accuracy and traceability of the experimental data. Based on the above data processing and verification procedure, the orthogonal experimental results of laser texturing for the three materials are summarized in Table 4.

Table 4. Orthogonal experimental results for the three PEEK-based materials

Experimental run number	PEEK5600G		PEEK5600LF30		PEEK5600CF30	
	Depth H1(um)	Width W1(um)	Depth H2(um)	Width W2(um)	Depth H3(um)	Width W3(um)
F1	2.7136	19.1875	9.8507	86.9146	18.1623	71.7152
F2	1.7923	17.445	6.2637	78.8422	22.6676	78.3968
F3	4.4715	21.2518	9.2091	91.7602	21.1382	70.3789
F4	3.489	22.1827	8.2919	95.1006	11.5577	65.2564
F5	5.7229	11.1803	7.8079	88.4191	12.5576	62.1384
F6	23.8793	13.6305	13.9309	123.1631	40.005	91.3143
F7	12.0351	31.943	18.3452	97.0004	28.0013	68.1509
F8	11.4127	17.0199	17.8771	94.6552	36.5132	71.7552
F9	2.3355	8.878	8.8972	79.9557	7.6836	61.6929
F10	6.5983	16.4828	12.8555	82.0917	16.2589	68.823
F11	5.7454	23.8624	28.4366	121.6041	51.6774	93.3189
F12	10.7953	30.2115	14.2859	83.3099	19.6651	74.3879
F13	8.6495	36.8381	17.8822	97.7732	37.8143	77.7826
F14	4.5691	21.2587	17.4773	92.2053	42.2849	75.056
F15	5.745	24.7695	9.2723	80.183	14.2551	70.3789
F16	26.3497	51.6621	23.5755	119.1765	75.5883	94.4323
F17	25.5308	45.4259	30.793	118.9314	82.9459	84.6329
F18	6.6893	32.3814	37.5822	93.9558	27.1313	81.962
F19	8.6572	33.5129	54.7542	94.5371	43.2978	85.5273
F20	2.6688	21.5881	10.8324	78.9641	10.8023	73.2742
F21	23.8752	49.4617	32.8833	106.6239	69.4459	92.428
F22	24.7863	40.662	31.4388	118.3323	90.0356	87.9376
F23	6.3476	30.6865	19.3881	88.7286	21.6046	78.1741
F24	14.4266	39.2946	45.1462	95.6462	44.5502	81.7375
F25	12.4924	45.5084	58.5626	91.3055	51.5649	82.6284

ISSN: 2414-1895 DOI: 10.6919/ICJE.202603_12(3).0043

2.5 Analysis of Orthogonal Experimental Results of Surface Texture Laser Processing

2.5.1 Depth Response Analysis

(1) Range analysis

Based on the L25 orthogonal experimental data for the three PEEK-based materials, the mean values of texture depth, (k), and the ranges, (R), were calculated for laser average power (P), scanning speed (v), and number of scans (n) at each level. The results are summarized in Table 1.

Table 5. Results of range analysis of texture depth for the three materials

Material	R_P/ μm	R_v/ μm	R_n/ μm	Order of influence
PEEK 5600G	12.748	9.867	9.216	$P > v \gtrsim n$
PEEK 5600CF30	29.199	7.047	15.412	$P > n > v$
PEEK 5600LF30	38.224	29.888	32.004	$P \gtrsim n \gtrsim v$

(2) Analysis of variance

Based on the range analysis, a three-factor ANOVA was conducted on the depth response of the three materials, and the F-values and p-values of each factor are summarized in Table 6 ($\alpha = 0.05$).

Table 6. Summary of ANOVA results for texture depth of the three materials

Material	Factor	F-value	P-value	Significance ($\alpha = 0.05$)
PEEK5600G	P	4.718	0.016	Significant
	v	4.210	0.023	Significant
	n	2.044	0.152	Not significant
PEEK5600CF30	P	6.657	0.0046	Significant
	v	0.383	0.816	Not significant
	n	1.576	0.244	Not significant
PEEK5600LF30	P	11.655	0.00043	Significant
	v	8.207	0.0020	Significant
	n	8.428	0.0018	Significant

Based on the results in Tables 5 and 6, laser power was the dominant factor affecting texture depth in all three PEEK-based materials. The range analysis indicated that the largest range in depth was always associated with the power factor, and ANOVA further confirmed its significant effect on depth for all materials. However, the sensitivity to the other parameters differed among materials. PEEK 5600CF30 depended mainly on laser power, with scanning speed and number of scans showing no significant effects, suggesting a relatively stable depth threshold. For PEEK 5600G, both laser power and scanning speed significantly affected depth. PEEK 5600LF30 was the most sensitive, with all three factors showing highly significant effects. These results indicate that increasing laser energy density is the key to increasing texture depth. However, for reinforced composites, especially PEEK 5600LF30, precise control of scanning speed and number of scans is also required for accurate depth regulation.

2.5.2 Width Response Analysis

(1) Range analysis

ISSN: 2414-1895 DOI: 10.6919/ICJE.202603_12(3).0043

Based on the L25 orthogonal experimental results for the three PEEK-based materials, the mean values of texture width, (k), and the ranges, (R), were calculated for laser average power (P), scanning speed (v), and number of scans (n) at each level. The results are summarized in Table 7.

Table 7. Range analysis results of texture width for the three materials

Material	R_P/ μm	R_v/ μm	R_n/ μm	Order of influence
PEEK5600G	23.532	9.232	10.234	$P \gg n \gtrsim v$
PEEK5600CF30	12.906	27.304	19.935	$v > n > P$
PEEK5600LF30	15.004	17.193	8.953	$v \gtrsim P > n$

(2) Analysis of variance

Based on the range analysis, a three-factor ANOVA was conducted on the width response to evaluate the effects of laser average power P, scanning speed v, and number of scans n. The resulting F-values and p-values are summarized in Table 8, with the significance level set at $\alpha = 0.05$.

Table 8. Summary of ANOVA results for texture width of the three materials

Material Material	Factor	F-value	P-value	Significance ($\alpha = 0.05$)
PEEK5600G	P	12.087	0.000359	Significant
	v	1.713	0.211627	Not significant
	n	2.125	0.140298	Not significant
PEEK5600CF30	P	1.951	0.166546	Not significant
	v	7.739	0.002530	Significant
	n	5.010	0.013115	Significant
PEEK5600LF30	P	19.177	0.000038	Significant
	v	18.751	0.000042	Significant
	n	6.390	0.005405	Significant

The results in Tables 7 and 8 indicate that the variation in texture width showed clear material dependence. For PEEK 5600G, laser power had the largest range, and ANOVA showed that only laser power was significant, indicating that the texture width was mainly governed by laser power. For PEEK 5600CF30, scanning speed showed the largest range, followed by the number of scans, and both factors were significant, suggesting that the texture width was mainly affected by scanning speed and number of scans. For PEEK 5600LF30, laser power, scanning speed, and number of scans were all significant, indicating high sensitivity to all three factors and a combined effect on width formation. Therefore, different materials require different parameter optimization strategies.

2.6 Morphological Characterization of Laser-Processed Materials and Analysis of Their Differential Response Mechanisms

Based on the range and ANOVA results of the L25 orthogonal experiments, four representative specimens, namely F13 (a), F15 (b), F20 (c), and F23 (d), were selected for in-depth analysis of microscopic morphology and mechanisms. These four parameter sets cover different combinations of energy density and thermal interaction time. Through cross-validation between macroscopic statistical data and microscopic morphology characterization, the regulatory mechanisms of laser

ISSN: 2414-1895 DOI: 10.6919/ICJE.202603_12(3).0043

power, scanning speed, and number of scans on the material removal behavior and surface quality of the three PEEK-based materials are revealed.

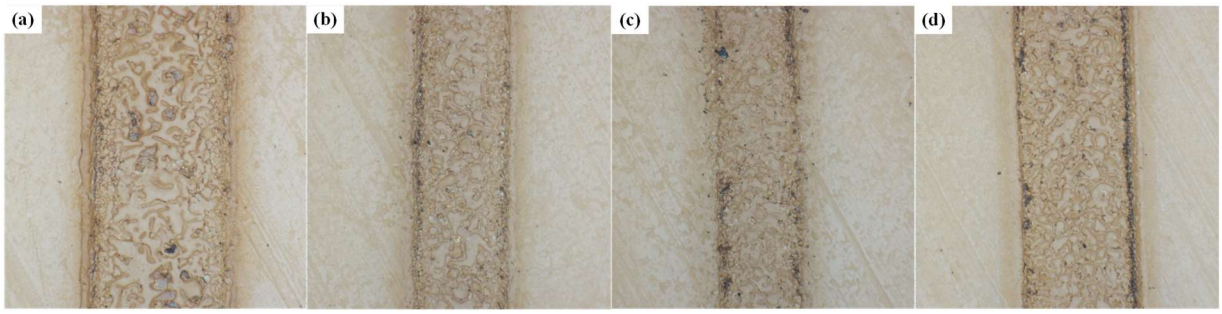

Figure 7. Laser-processed samples of PEEK5600G F13(a); F15(b); F20(c); F23(d)

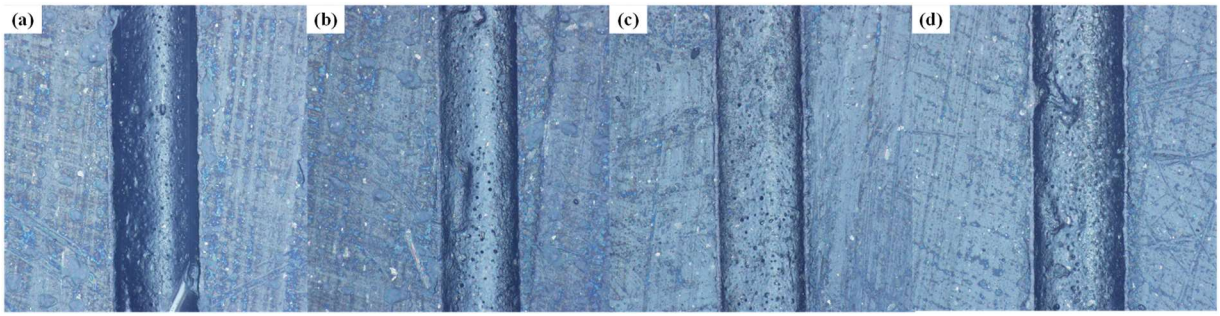

Figure 8. Laser-processed samples of PEEK5600LF30 F13(a); F15(b); F20(c); F23(d)

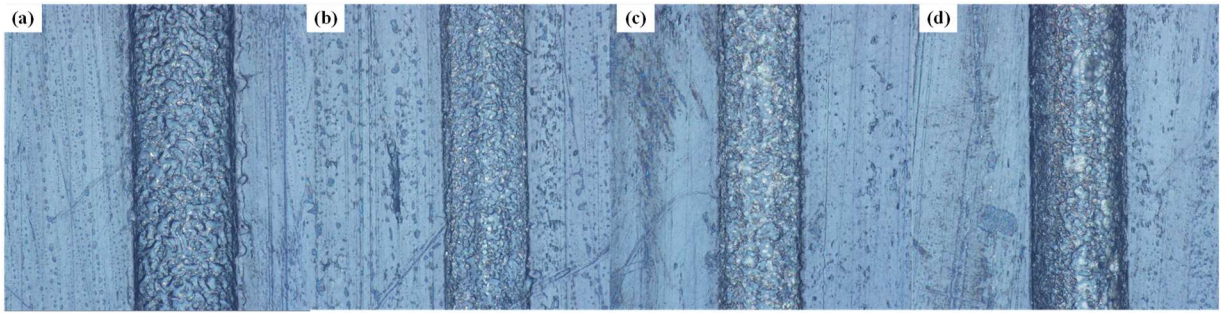

Figure 9. Laser-processed samples of PEEK5600CF30 F13(a); F15(b); F20(c); F23(d)

(1) Competitive ablation–melting mechanism and edge effect

Comparison of the microscopic morphologies of the three PEEK-based materials under different processing parameters (Figs. 7–9a–d) showed that all specimens exhibited typical photothermal removal features. Specifically, the central region of the groove was a vaporization-dominated removal zone under high energy density, whereas the groove edges were accompanied by different degrees of recast layers and material accumulation. This phenomenon clearly indicates that ablation and melting coexisted as competing removal mechanisms during femtosecond laser processing of PEEK-based materials. In the edge region of the Gaussian laser beam, the energy density was lower than the vaporization threshold of the material but still higher than its melting point, causing thermal softening and melting of the matrix. Driven by recoil pressure and the Marangoni effect, the molten material flowed toward both sides of the groove and accumulated there, forming edge bulges after cooling. This interpretation was strongly supported by the range analysis. The presence of ridge height was not an accidental error, but a direct reflection of the degree of thermal accumulation. In particular, specimen a (80 mm/s) with a lower scanning speed showed more pronounced edge accumulation than

ISSN: 2414-1895 DOI: 10.6919/ICJE.202603_12(3).0043

specimen b (120 mm/s). ANOVA further confirmed that scanning speed was a significant factor affecting ridge height in all three materials, indicating that the edge effect was mainly controlled by the thermal interaction time of the laser spot. Therefore, ridge height should be included as a key evaluation index for characterizing thermal damage.

(2) Morphological differentiation caused by compositional differences

Although the processing parameters were the same, the texture morphologies of the three materials showed significant material dependence, which was mainly attributed to differences in thermophysical properties caused by compositional variation. As a pure resin matrix, PEEK 5600G exhibited relatively rounded and continuous edge contours in specimens a–d. Because no reinforcing phase was present to hinder melt flow, the molten matrix showed better fluidity, and the recast layer formed after cooling was relatively uniform. Combined with the ANOVA results, its width was significantly affected only by laser power, indicating that its material removal process was relatively simple and mainly governed by energy density. In contrast, PEEK 5600CF30 exhibited the most complex morphology. Especially in specimens a and d, the groove inner walls were rough, and obvious nodular protrusions were observed at the edges. This is because carbon fiber, with its high thermal conductivity and high vaporization point, acted as a thermal channel during processing, rapidly conducting heat along the fiber axis and thereby causing lateral expansion of the heat-affected zone. This mechanism explains why, in the width ANOVA results, CF30 was the only material for which scanning speed was significant while laser power was not, indicating that its width formation no longer depended solely on laser spot energy input, but more on the time available for heat diffusion along the fibers. By contrast, PEEK 5600LF30 contains lubricating components such as PTFE, whose decomposition temperature differs from that of the matrix. Local micro-explosions or gas release were therefore likely to occur during processing, leading to poor morphological integrity under high-energy-input conditions such as specimen a. Statistically, this was reflected in its high sensitivity to all processing parameters and its narrowest processing window.

3. Conclusion

(1) The groove depth of all three PEEK-based materials was mainly governed by laser power, although their sensitivities to the secondary parameters differed. The depth of PEEK5600G was significantly affected by laser power and scanning speed, that of PEEK5600CF30 was mainly affected by laser power, and PEEK5600LF30 was sensitive to laser power, scanning speed, and number of scans, indicating that its machining process responded more strongly to variations in energy input.

(2) Groove width showed clear material dependence. The width of PEEK5600G was mainly controlled by laser power, that of PEEK5600CF30 was mainly affected by scanning speed and number of scans, and PEEK5600LF30 was sensitive to all three parameters. These results indicate that different reinforcing components can significantly influence the lateral heat diffusion behavior and edge formation characteristics of the materials.

(3) All three PEEK-based materials exhibited a competitive ablation–melting mechanism under femtosecond laser irradiation. Ablation dominated in the central region of the groove, whereas recast layers and molten accumulation tended to form at the edges. With increasing thermal input, groove depth and profile clarity improved, but edge thermal damage also became more severe. Therefore, process optimization should balance target dimensions and edge quality, and a comprehensive evaluation principle of “meeting dimensional requirements while keeping defects under control” should be established.

Acknowledgments

This work was supported by Basic Research on the National Major Special Project for Aero Engines and Gas Turbines (No. Y2022-IV-0001-0018), the Youth Innovation Team of Shaanxi Universities

ISSN: 2414-1895 DOI: 10.6919/ICJE.202603_12(3).0043

(2025), and the Qinchuangyuan “Scientist + Engineer” Team Development Project of Shaanxi Province (No. 2024QCY-KXJ-112).

References

[1] X.Z. Xue, S.M. Wang and B. Li: Modification methodology of fretting wear in involute spline, Wear, vol. 368-369 (2016), p.435-444.

[2] Y. Yuan, G. Zhao, X. Zhao, et al.: Contact stress prediction and fretting wear measurement of aeronautic crowned involute splines, Tribology International, vol. 193 (2024), 109407.

[3] X. Zhang, Z. Yao, H. Du, J. Song, Z. Jin and W. Xu: Wettability and frictional studies of PEEK composites against Co-Cr alloys with surface textures, Polymers, vol. 15 (2023) No. 19, 4006.

[4] X.H. Zheng, H. Song, Q. Zhang, et al.: Research progress on the influence of laser surface texturing on the tribological properties of materials, Materials Review, vol. 31 (2017) No. 17, p.68-74.

[5] X.R. Song, S.J. Li, Y.Y. Hou, Z.W. Ba, H.Y. Zheng and M.M. Liu: Research progress on the influence of laser texturing on the tribological properties of material surfaces, Materials Protection, vol. 56 (2023) No. 10, p.25-41.

[6] I. Etsion: State of the art in laser surface texturing, Journal of Tribology, vol. 127 (2005) No. 1, p.248-253.

[7] C. Gachot, A. Rosenkranz, S.M. Hsu, et al.: A critical assessment of surface texturing for friction and wear improvement, Wear, vol. 372-373 (2017), p.21-41.

[8] Z.H. Chen: Study on the mechanism of laser micro-texture modification and meshing characteristics of space gear surfaces (Jiangsu University, Jiangsu, China 2023).

[9] A. Riveiro, R. Soto, R. Comesaña, M. Boutinguiza, J. del Val, F. Quintero, F. Lusquiños and J. Pou: Laser surface modification of PEEK, Applied Surface Science, vol. 258 (2012) No. 23, p.9437-9442.

[10] M.Y. Cui, J.S. Wei, R.S. Xiao, T. Huang, et al.: Femtosecond laser modification-assisted electroless copper plating on polyetheretherketone surface, Surface Technology, vol. 54 (2025) No. 24, p.98-105.

[11] T.X. Liu, J. Li, X. Lu, et al.: Effect of laser surface texturing parameters on the tribological properties of steel ball-steel disc under starved lubrication, Lubrication Engineering, vol. 48 (2023) No. 7, p.74-80.

[12] M. Hintze, N. Eliasen and I. Sivebaek: Wear and friction of PEEK composites, dry or lubricated, Wear, vol. 534-535 (2023), 205135.

[13] A.A. Seenath, M.M.A. Baig, J.K. Katiyar, et al.: A comprehensive review on the tribological evaluation of polyether ether ketone pristine and composite coatings, Polymers, vol. 16 (2024) No. 21, 2994.

[14] S. Hammouti, B. Beaugiraud, M. Salvia, et al.: Elaboration of submicron structures on PEEK polymer by femtosecond laser, Applied Surface Science, vol. 327 (2015), p.277-287.

[15] S. Hammouti, A. Pascale-Hamri, N. Faure, et al.: Wear rate control of PEEK surfaces modified by femtosecond laser, Applied Surface Science, vol. 357 (2015), p.1541-1551.

[16] P.Y. Zhu: Study on the friction performance of groove micro-texture on spur gears (Xiamen University of Technology, Xiamen, China 2021).

[17] A. Wilson, I. Jones, F. Salamat-Zadeh, et al.: Laser surface modification of poly(etheretherketone) to enhance surface free energy, wettability and adhesion, International Journal of Adhesion and Adhesives, vol. 62 (2015), p.69-77.

[18] Y.Y. Yu, Y.M. Hu, X.M. Dai, et al.: Analysis and parameter optimization of fretting wear in spline pairs, Mechanical Science and Technology for Aerospace Engineering, vol. 40 (2021) No. 6, p.828-834.

[19] A. Riveiro, A.L.B. Maçon, J. del Val, R. Comesaña and J. Pou: Laser surface texturing of polymers for biomedical applications, Frontiers in Physics, vol. 6 (2018), 16.

[20] M.M. Omrani, A. Hadjizadeh, A. Milani and K. Kim: PEEK surface modification methods and effect of the laser method on surface properties, Bio-Interface Research in Applied Chemistry, vol. 10 (2020) No. 3, p.5132-5140.

[21] S. Sasaki: Surface texturing for friction control: A review on existing technology and prospects, Tribology Online, vol. 19 (2024) No. 2, p.105-120.

ISSN: 2414-1895 DOI: 10.6919/ICJE.202603_12(3).0043

[22] A.F. Obilor, M. Pacella, A. Wilson and V.V. Silberschmidt: Micro-texturing of polymer surfaces using lasers: a review, The International Journal of Advanced Manufacturing Technology, vol. 120 (2022), p.103-135.

[23] L. Yang, W. Ma, F. Gao and S. Xi: Effect of groove width on micromachine groove texture tribology characteristics of 0Cr17Ni7Al, Coatings, vol. 12 (2022) No. 8, 1221.